



# Divergent Trends of Black and Brown Carbon Driven by Anthropogenic Emissions and Open Biomass Burning Across Asia

Ying Zhang<sup>1,2</sup>, Abudurexiati Abulimiti<sup>2</sup>, Yan-Lin Zhang<sup>2</sup>

<sup>1</sup>State Key Laboratory of Climate System Prediction and Risk Management/Key Laboratory of Meteorological Disaster, Ministry of Education/Collaborative Innovation Center on Forecast and Evaluation of Meteorological Disasters, School of Atmospheric Sciences, Nanjing University of Information Science and Technology, Nanjing, 210044, China

<sup>2</sup>School of Ecology and Applied Meteorology, Nanjing University of Information Science and Technology, Nanjing, 210044, China

Correspondence to: Yan-Lin Zhang ([zhangyanlin@nuist.edu.cn](mailto:zhangyanlin@nuist.edu.cn) or [dryanlinzhang@outlook.com](mailto:dryanlinzhang@outlook.com))

**Abstract.** Black carbon (BC) and brown carbon (BrC) are the dominant light-absorbing carbonaceous aerosols (LACs) and contribute substantially to regional climate warming. Across Asia, heterogeneous changes in anthropogenic and open biomass burning (OBB) emissions driven by clean air policies and climate variability are reshaping LAC composition, yet how these changes alter the relative abundance and radiative roles of BC and BrC remains poorly understood. Here, using the chemical transport model GEOS-Chem combined with machine-learning attribution, we quantify the responses of BC and BrC to concurrent emission changes across East, South, and Southeast Asia during 2012–2019. We identify pronounced spatial heterogeneity in BrC/BC mass ratio trends. East Asia exhibits a significant upward trend, driven by policy-induced suppression of BC-rich anthropogenic sources alongside enhanced BrC-rich OBB from a seasonal shift in crop residue burning under open-fire regulations. In contrast, South and Southeast Asia show declining ratios attributable to residential energy transitions and wildfire variability, respectively. These asymmetric responses propagate into direct radiative forcing (DRF), with the DRF<sub>BrC</sub>/DRF<sub>BC</sub> ratio increasing from 34.1% to 41.3% in East Asia while declining elsewhere. Notably, in East and Southeast Asia, OBB amounts to up to half of anthropogenically driven radiative forcing changes. Our results demonstrate that emission mitigation can redistribute rather than proportionally reduce LAC warming, highlighting that future climate benefits will critically depend on the concurrent management of open biomass burning.

## 15 1 Introduction

Light-absorbing carbonaceous aerosols (LACs), strongly influence the radiative balance of the Earth system by directly absorbing solar radiation (Bond et al., 2013; Saleh, 2020) or indirectly altering cloud and precipitation processes (Liu et al., 2020). LACs consist of black carbon (BC), which strongly absorbs solar radiation throughout the entire spectrum (Bond et al., 2013), and brown carbon (BrC), a component of organic carbon (OC) characterized by wavelength-dependent absorption from visible to ultraviolet range (Saleh, 2020). Of the two, BC is the primary contributor to the radiative effect of LACs, with a global direct radiative forcing (DRF) due to aerosol-radiation interaction ranging from 0.21 to 0.39 W m<sup>-2</sup> (Thornhill

et al., 2021; Tuccella et al., 2020; Zhang et al., 2020), higher than that of BrC (0.03–0.22 W m<sup>-2</sup>) (DeLessio et al., 2024; Drugé et al., 2022; Saleh et al., 2015; Zhang et al., 2020).

BC is a direct product of incomplete fuel combustion, with major sources from anthropogenic activities (e.g., industry, power generation, transportation, and residential combustion) and open biomass burning (OBB; e.g., forest, shrub, and crop residue fires) (Hoesly et al., 2018; Pan et al., 2020). In contrast, though sharing similar sources, primary BrC (BRpri) predominantly originates from OBB and residential solid fuel combustion (Atwi et al., 2022; Satish et al., 2020; Xiong et al., 2022). Additionally, BrC can be formed secondarily via the oxidation of volatile organic compounds (VOCs), termed secondary BrC (BRsec) (Liu et al., 2015; Siemens et al., 2022). These source-level discrepancies thus imply that BC and BrC may respond differently to profound shifts in emission regimes, driven by anthropogenic mitigation (Geng et al., 2024; McDuffie et al., 2020) and climate-sensitive wildfires (Jones et al., 2022).

Asia, as one of the largest source regions of LACs globally, has undergone pronounced and spatially heterogeneous shifts in emission regimes over the past decade, particularly in East, South and Southeast Asia. This makes it a natural laboratory for examining how divergent anthropogenic and OBB trajectories reshape LACs. In East and South Asia, LACs' sources are dominated by anthropogenic activities, with China and India accounting for nearly 50% of global anthropogenic carbonaceous aerosol emissions (McDuffie et al., 2020; Xu et al., 2021). In both regions, OBB is also predominantly from human agricultural activities (Gong et al., 2025; Yin, 2020). Since 2013, East Asia, especially China, has achieved substantial reductions in both anthropogenic emissions and harvest-season open burning, driven by stringent air pollution controls and straw burning bans (Geng et al., 2024; Kurokawa and Ohara, 2020; You et al., 2026). Meanwhile, South Asia has seen relatively modest changes, as the rollout of clean energy and open burning controls has faced socioeconomic and infrastructural constraints (Bhuvaneshwari et al., 2019; Roy, 2024). Southeast Asia, by contrast, stands out as a wildfire-prone region (Pan et al., 2020; Yadav et al., 2017), with anthropogenic emission intensities considerably lower than those in East and South Asia (Kurokawa and Ohara, 2020). Emissions of LACs in this region are primarily from natural open burning, which is highly sensitive to climate variability and thus exhibits strong interannual fluctuations (Chen et al., 2017; Yin et al., 2021).

Therefore, East, South, and Southeast Asia represent three real-world emission trajectories: policy-driven, near-baseline transition and climate-sensitive, respectively. These heterogeneous trajectories are likely to drive regionally distinct responses of BC and BrC. Both observational and modeling studies have demonstrated that BC is generally expected to decline under policy controls over Asia (Liu et al., 2022a; Pathak et al., 2024; Xie et al., 2025; Zheng et al., 2025), while the response of BrC remains poorly constrained. An unresolved question is therefore whether anthropogenic mitigation together with OBB variability reshapes LACs uniformly, or instead alters the relative abundance and radiative importance of BC and BrC across regions.

To address this question, we investigate emission-driven changes in the BrC/BC mass ratio across Asia from 2012 to 2019 and identify the key contributors using the chemical transport model GEOS-Chem combined with Shapley Additive exPlanations (SHAP). We then quantify how these changes affect the contributions of BC and BrC to the DRF of LACs.



This provides insight into how evolving emission patterns alter the balance of abundance and radiative forcing between these two species, with implications for targeted mitigation strategies. This paper is organized as follows. Section 2 describes the model setup and observational data. Section 3 presents model evaluation, analyzes BrC/BC trends, and discusses the underlying drivers. Section 4 presents the conclusions.

## 60 **2 Methodology**

### **2.1 Model and simulation**

#### **2.1.1 Model description**

The GEOS-Chem model (version 13.2.0, <http://10.5281/zenodo.5500536>) was used in this study to simulate aerosol mass for 2012 to 2019 after a 4-month spin up. The simulation was run at a resolution of  $2^{\circ} \times 2.5^{\circ}$  with 47 vertical layers  
65 driven by MERRA2 assimilated meteorology. The study area comprises East, South, and Southeast Asia and their surroundings (Fig. S1).

Anthropogenic emissions were taken from the Community emissions Data System (CEDS, v2021\_04\_21 release; Hoesly et al., 2018), while emissions of gaseous species in China were overwritten by Multi-resolution Emission Inventory for China (MEIC) version 1.3 (Zheng et al., 2018). The SO<sub>2</sub> emission from MEIC is scaled up by a factor of 1.5 (Koukouli et al., 2018). OBB emissions were taken from Fire Energetics and Emissions Research (FEER) version 1.0 (Ichoku and Ellison, 2014). The injection height was treated by distributing OBB emissions uniformly within the boundary layer, following Pan et al. (2020). Biogenic emissions were calculated online by MEGAN version 2.1 (Guenther et al., 2012).  
70

#### **2.1.2 Simulation of BC and BrC**

In GEOS-Chem, the parameterizations of BC and primary OC follow Park et al. (2003). The formation of secondary OC (SOC) is based on an irreversible scheme with fixed yields (Kim et al., 2015). We isolated the BrC from OC. Both BRpri and BRsec were considered.  
75

Two dominant sources of BRpri, OBB and residential solid fuel combustion, were included; and their emissions were obtained via multiplying OC emissions (from inventories) by the mass ratio  $M_{BRpri}/M_{OC}$ . This ratio was derived by linking BRpri emission to its absorption, based on an empirical relationship between combustion efficiency and absorption  
80 Angstrom exponents (Jo et al., 2016). Details are provided in Text S1 and Table S1. This approach estimates the global BRpri emissions at 5.40 Tg C yr<sup>-1</sup> for OBB and at 3.18 Tg C yr<sup>-1</sup> for residential sources, in good agreement with bottom-up estimates (Xiong et al., 2022; Table S2). For BRsec, we considered only SOC formed from anthropogenic aromatic VOCs (AVOC) to be light-absorbing, as treated previously (Xu et al., 2024; Zhang et al., 2020); while SOC from other sources (e.g., biogenic VOCs), due to its negligible absorption (Liu et al., 2015), was not considered.



85 The optical calculations of BC and BrC (adopting treatments of scattering OC) were based on the aerosol optical  
scheme in GEOS-Chem (Martin et al., 2003), with following modifications. The refractive index of BC was updated to  $1.95$   
 $+ 0.79i$  at 550 nm (Bond and Bergstrom, 2006). The imaginary refractive index of BRpri and BRsec (Table S3) were  
obtained from field observations of OBB (Kirchstetter et al., 2004) and laboratory measurements of aromatic SOC (Liu et al.,  
2015), respectively. Given the significant variability in BrC photobleaching rates (Qiu et al., 2024, 2026; Wong et al., 2017),  
90 this process was not considered in our study. Both BrC and scattering OC were converted to organic matter using a factor of  
2.1 (Park et al., 2003).

### 2.1.3 DRF calculation

Shortwave DRF of BC and BrC were estimated under clear-sky condition using the shortwave component of Rapid  
Radiative Transfer Model for GCMs (RRTMG\_SW, [https://github.com/AER-RC/RRTMG\\_SW](https://github.com/AER-RC/RRTMG_SW)). Here, DRF refers to  
95 radiative forcing directly induced by the aerosol-radiation interaction (IPCC, 2021). This model simulates the net solar flux  
at the top of atmosphere (TOA) across 14 spectral bands ranging from 0.2 to 12.2  $\mu\text{m}$  (Iacono et al., 2008). The BrC  
absorption-induced DRF was calculated as the difference between two RRTMG\_SW runs, one with BrC absorption  
(including BRpri and BRsec) and one without. In other words, the effect of BrC scattering was not considered. The BC DRF  
was calculated in the same way, except that the small effect of its scattering was included.

### 100 2.2 Trend analysis

Trends in BC, BrC and the BrC/BC ratio were derived from monthly simulation outputs using Seasonal-Trend  
decomposition with Loess (STL) (Cleveland et al., 1990) combined with linear regression. Specifically, the time series data  
were first decomposed into trend ( $T_i$ ), seasonal ( $S_i$ ), and residual ( $R_i$ ) components using STL. Linear regression was then  
performed on  $T_i$ , with the slope representing the long-term trend. This approach is advantageous as it isolates long-term trend  
105 from seasonal fluctuations and short-term anomalies, and has therefore been widely used in atmospheric sciences (Biswal et  
al., 2025; Li et al., 2014; Xu et al., 2023a). It enables a robust assessment of long-term changes in the mass and DRF of BC  
and BrC, along with their corresponding BrC/BC ratios.

### 2.3 Random forest and SHAP analysis

A random forest (RF) statistical model, coupled with Shapley Additive exPlanations (SHAP), was used to investigate  
110 the contributors of BC, BrC and their mass ratio. RF captures the non-linear responses of these target variables to emissions  
and meteorology, while SHAP provides feature attribution. This approach is widely used to attribute multiple predictors in  
atmospheric science (Dai et al., 2023; Hou et al., 2022; Wang et al., 2024).

Here, we first built the RF models separately for each target variable (i.e., BC, BrC, and the BrC/BC ratio) with the  
following inputs: meteorological variables (temperature, pressure, relative humidity, 10 m wind components) from GEOS-  
115 Chem, and emissions of BC, BRpri and AVOC (precursors of BRsec) from inventories. The dataset was randomly split into



training (80%) and testing (20%) sets. The RF model was trained on the training set, with hyperparameters optimized by 10-fold cross-validation to maximize the mean  $R^2$ . The optimized model was then evaluated on the unseen test set. Subsequently, SHAP was used to interpret the contributions of anthropogenic and OBB emissions, and meteorology.

## 2.4 Observations

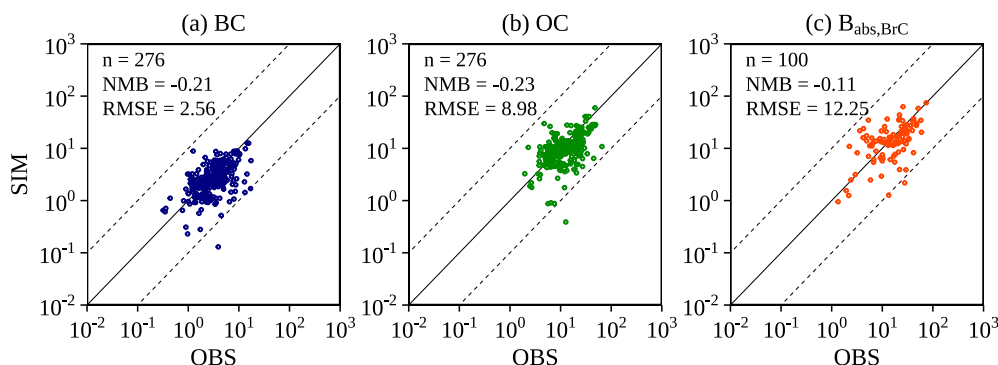
120 Surface observations over East, South and Southeast Asia were collected for model evaluation. Locations of  
observational sites are shown in Fig. S1. The mass concentrations of BC and OC were compiled from short-term  
observations at multiple sites (Table S4) and long-term monitoring in Beijing (Ji et al., 2019; Sun et al., 2022), Nanjing  
(Abulimiti et al., 2025) and Fukue (Kanaya et al., 2020). Here, OC denotes the sum of BrC and scattering OC due to lacking  
direct measurements of BrC concentration. These data were used to evaluate the model performance in simulating BC and  
125 OC concentrations and their long-term variations. In addition, the absorption of OC measured at 365–370 nm was collected  
to evaluate the simulated BrC absorption, including short-term site observations (Table S5) and long-term observations in  
Nanjing (Chen et al., 2019; Xie et al., 2020; Text S2).

## 3. Results and Discussion

### 3.1 Model evaluation

130 We first evaluated the simulated BC and OC mass concentrations against observations across East and Indo-Southeast  
Asia. See Sect. 2.4 for details of observations. The model reproduced the observed levels well, with normalized mean biases  
(NMB) within  $\pm 0.25$  (Figs. 1a–1b). Notably, it also successfully captured the long-term trends of BC and OC at urban sites  
(Beijing and Nanjing), as well as the BC trend at the background site Fukue (OC was not available) (Figs. S2a–S2e). The  
model thus reliably captures concentration trends in various environments, from emission-dominated urban areas to  
135 transport-influenced background sites. Furthermore, in the absence of BrC mass concentration data, we evaluated the model  
by comparing the simulated BrC absorption ( $B_{\text{abs,BrC}}$ ) with OC absorption measurements (details in Sect. 2.4). The simulated  
 $B_{\text{abs,BrC}}$  at 370 nm showed good agreement with observed values (NMB:  $-0.11$ ; Fig. 1c), and its long-term trend in Nanjing  
was consistent with local observations (Fig. S2f).

Overall, the simulated results demonstrate reasonable accuracy in both the magnitudes and long-term trends of BC and  
140 OC concentrations, along with BrC absorption, providing a reliable basis for subsequent analysis of trends in BrC/BC ratios  
and their radiative forcing implications.

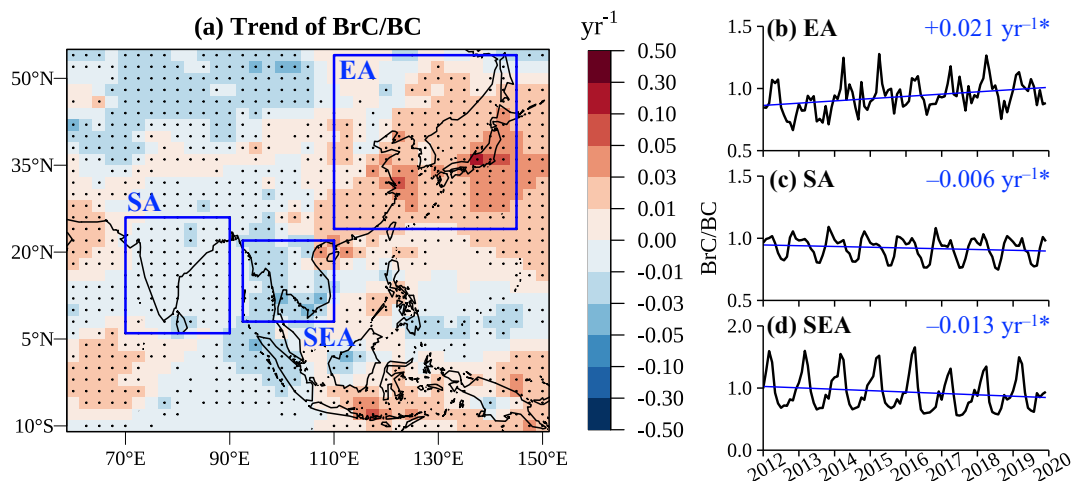


145 **Figure 1.** Comparison between simulations (SIM) and observations (OBS): (a) BC and (b) OC mass concentrations (unit:  $\mu\text{g m}^{-3}$ ), (c) BrC absorption ( $B_{\text{abs,BrC}}$ ) at 370 nm (unit:  $\text{M}\cdot\text{m}^{-1}$ ). Number of data (n), normalized mean bias [ $\text{NMB} = \sum(\text{SIM} - \text{OBS}) / \sum \text{OBS}$ ] and root mean squared error [ $\text{RMSE} = \sqrt{(\sum(\text{SIM} - \text{OBS})^2 / n)}$ ] are shown inset.

### 3.2 Spatiotemporal trend of BrC/BC

During 2012–2019, the trends in BrC/BC mass ratio exhibited distinct spatial heterogeneity across Asia, particularly in East, South and Southeast Asia (Fig. 2a, regions outlined by blue rectangles), despite their comparable mean ratios (Fig. S3). This distinct pattern highlights the divergent responses of BC and BrC to localized variations in anthropogenic emissions and  
150 OBB activities.

East Asia, representing a policy-driven regime, experienced a statistically significant positive trend of  $+0.021 \text{ yr}^{-1}$  ( $p < 0.05$ ; Fig. 2b), corresponding to a relative increase of 14.3% when compared to its multi-year mean BrC/BC of 1.03. This reflects a systematic rise in the relative contribution of BrC to total LACs concentrations under stringent air pollution controls. By contrast, South (near-baseline transition regime) and Southeast Asia (climate-sensitive regime) showed negative  
155 trends of  $-0.006$  and  $-0.013 \text{ yr}^{-1}$ , respectively (both  $p < 0.05$ ; Figs. 2c–2d). Relative to their multi-year mean BrC/BC of 0.92 (South Asia) and 0.97 (Southeast Asia), these trends translate to relative reductions of 4.6% and 9.4%, respectively. These contrasting results arise from the different emission trajectories across these three regions, whose underlying drivers will be discussed in detail below using trend and SHAP analysis. The optimized hyperparameters and performance metrics of RF statistical models, which were built to support the SHAP analysis, are presented in Table S6.



160

**Figure 2.** (a) Trends in the BrC/BC mass ratio across Asia for 2012–2019, with dots indicating statistical significance ( $p < 0.05$ ). East Asia (EA), South Asia (SA) and Southeast Asia (SEA) are outlined by blue rectangles. (b–d) Regional mean BrC/BC (black) and corresponding trend (blue), with slope and statistical significance ( $p < 0.05$ , denoted by \*) shown inset.

### 3.2.1 East Asia

165

We first examine East Asia, where the BrC/BC ratio increased despite reductions in both BC and BrC concentrations. This upward trend was driven by a disproportionately faster decline in BC ( $-0.037 \mu\text{g m}^{-3} \text{yr}^{-1}$ ) compared to BrC ( $-0.011 \mu\text{g m}^{-3} \text{yr}^{-1}$ ) (Fig. 3a; see Figs. S4a–S4b for time series and source-specific trends). This disparity reflects an unintended consequence of targeted controls on anthropogenic emissions and agricultural open burning.

170

On one hand, clean air actions targeting fossil fuel used in industry and power generation (Geng et al., 2024; Zheng et al., 2018) have reduced BC more rapidly than BrC. We estimated a rapid decline of  $-0.049 \mu\text{g m}^{-3} \text{yr}^{-1}$  in anthropogenic BC (Fig. S4a), consistent with the observed trend of  $-0.06 \mu\text{g m}^{-3} \text{yr}^{-1}$  in China from 2007 to 2019 (He et al., 2023). In contrast, the decline in anthropogenic BrC (i.e., the sum of BRsec and residential BRpri) was considerably slower ( $-0.039 \mu\text{g m}^{-3} \text{yr}^{-1}$ ; Fig. S4b), owing to the relatively weaker reduction in residential combustion and VOC emissions (Geng et al., 2024; Li et al., 2023).

175

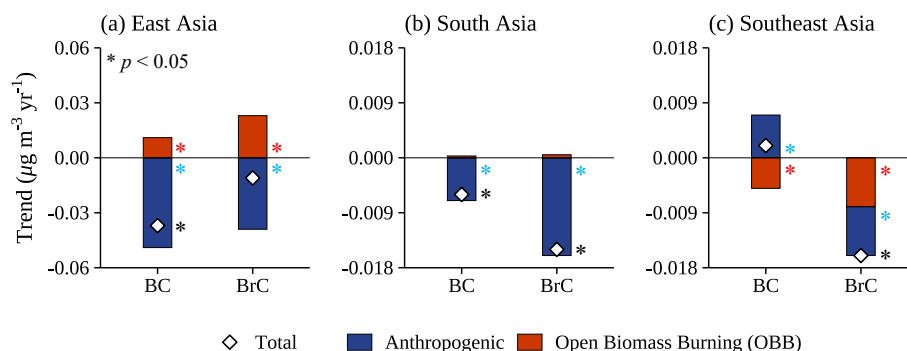
On the other hand, the unexpected increase in agricultural open burning partially offset these anthropogenic reductions, with a greater effect on BrC than BC (Fig. 3a), thus further widening the disparity in their decline rates. Open burning of crop residue accounts for 60%–80% of total OBB emissions in East Asia, especially in northeastern China (Gong et al., 2025; Liu et al., 2022b; Wang et al., 2020). Although straw burning bans in China have effectively reduced harvest-season burning (Wang et al., 2020; You et al., 2026), satellite observations reveal that open burning still intensifies in winter and spring (Dong et al., 2024; Wang et al., 2020; You et al., 2026). Our simulations captured this seasonal feature (Figs. S5a–S5b), consistent with satellite-retrieved burned area (Chen et al., 2023). Due to its lower combustion efficiency, which favors BrC emission over BC (Wang et al., 2022), the OBB-driven increase in BrC ( $+0.023 \mu\text{g m}^{-3} \text{yr}^{-1}$ ; Figure S4a) was approximately

180

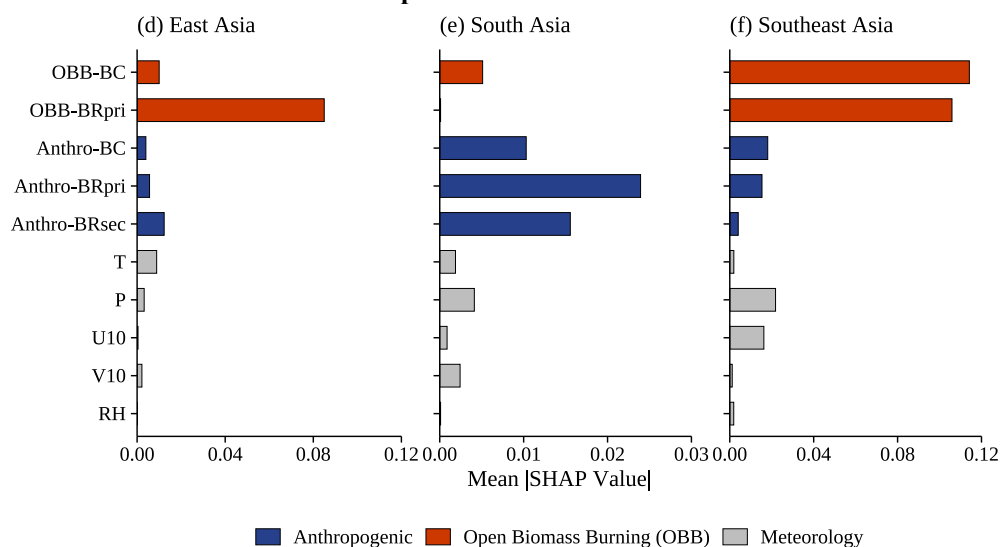
twice that of BC (+0.011  $\mu\text{g m}^{-3} \text{yr}^{-1}$ ; Fig. S4b). This growing contribution of OBB to BrC is further supported by a latest inventory (Zhou et al., 2026).

185 Consequently, reduction of anthropogenic emissions under air quality regulations, together with concurrent rise in OBB emissions driven by the seasonal redistribution of agricultural burning in response to open-fire restriction policies, results in greater relative BrC abundance in East Asia. The former suppresses BC-rich emissions, whereas the latter enhances BrC-rich emissions, as revealed by SHAP analysis (Figs. S6a–S6b). The meteorological influence was also investigated, which turned out to be relatively minor (Figs. S6a–S6b). Among these, OBB emissions driven by human agricultural activities serve as a  
 190 more critical factor, with far higher importance of BRpri emissions from OBB than other factors (Fig. 3d). These findings highlight the importance of season-specific strategies for managing agricultural open burning.

### Trends in BC and BrC Mass Concentrations



### Relative Importance of Different Factors



195 **Figure 3.** (a-c) Regional Trends in BC and BrC mass concentrations. Anthropogenic BrC is the sum of BRsec and residential BRpri. Asterisks (\*) denote the statistical significance ( $p < 0.05$ ) for total (black), anthropogenic (skyblue) and OBB (red) sources. (d-f) Relative importance of emissions (anthropogenic and OBB) and meteorological variables (T: temperature; P: pressure; U10: 10 m zonal wind; V10: 10 m meridional wind; RH: relative humidity).



### 3.2.2 South Asia

Despite modest overall emission reductions, South Asia exhibited a declining BrC/BC ratio, driven primarily by asymmetric decreases in anthropogenic BC and BrC (Fig. 3b). In contrast to East Asia, air quality management in South Asia has targeted residential combustion through the promotion of clean household fuels (Roy, 2024). Residential biofuel combustion, the dominant contributor to ambient PM<sub>2.5</sub> in South Asia (approximately 52%–68%; Reddington et al., 2019), emits BrC preferentially over BC due to its lower combustion efficiency. As a result, the growing use of clean cooking fuels (Gould and Urpelainen, 2018; Roy, 2024) has led to a much larger reduction in BrC ( $-0.016 \mu\text{g m}^{-3} \text{ yr}^{-1}$ ; Fig. S4c) than in BC ( $-0.007 \mu\text{g m}^{-3} \text{ yr}^{-1}$ ; Fig. S4d), thereby driving the BrC/BC mass ratio downward. This is consistent with a recent modeling study, which similarly found a larger decline in OC than BC driven by residential combustion reductions (Chatterjee et al., 2023). Nevertheless, the adoption of these policies remains challenging due to high costs, weak supply chains, and a habitual reliance on traditional fuels (Roy, 2024; Sharma and Dash, 2022). Therefore, the anthropogenically driven declines in BC and BrC over South Asia are much smaller than those in East Asia (Figs. S4a–S4d).

Moreover, trends in OBB-emitted BC and BrC were negligible and statistically insignificant (Figs. 3b and S4c–S4d). Similar to East Asia, the dominant source of OBB in South Asia is crop residue burning (Yin, 2020). However, due to high costs and difficulties in crop residue collection (Bhuvaneshwari et al., 2019), agricultural open burning remains at stable emission levels without significant declining trends (Majumdar, 2023; Yin, 2020). Consequently, only minor declines were simulated for OBB-emitted BC and BrC in South Asia.

The SHAP analysis also highlights the key role of anthropogenic emissions in modulating BC and BrC mass concentrations and their ratio in South Asia, with their importance exceeding those of open burning and meteorology (Figs. 3e and S6c–S6d). Our results indicate that reductions in residential emissions, even relatively modest, could induce a clear shift in the BrC/BC mass ratio in South Asia. These findings further imply that the BrC/BC mass ratio is more sensitive to source-specific emission changes than to the overall magnitude of emission reductions.

### 3.2.3 Southeast Asia

Southeast Asia also exhibited a decreasing BrC/BC ratio, resulting from a slightly increasing BC and a decreasing BrC (Fig. 3c). In this wildfire-prone region, both BC and BrC are strongly susceptible to climate-driven variability in natural open burning. Tropical wildfires are highly sensitive to the El Niño/Southern Oscillation (ENSO) (Chen et al., 2017). El Niño events intensify regional drought and promote fire activity, while La Niña events bring anomalously wet conditions that suppress OBB emissions. This ENSO-driven variability caused a substantial drop in OBB emissions in Southeast Asia during the 2017–2018 La Niña event (Hu et al., 2025; Huang et al., 2024), leading to lower BC and BrC. Our simulations well captured this feature (Fig. S5c), showing good agreement with satellite-retrieved burned area (Chen et al., 2023). The SHAP analysis also confirms OBB as the dominant factor in modulating BC and BrC concentrations in Southeast Asia (Figs.



S6e–S6f). Given the lower combustion efficiency of OBB, a larger decline occurred in BrC ( $-0.008 \mu\text{g m}^{-3} \text{yr}^{-1}$ ; Fig. S4f) than BC ( $-0.005 \mu\text{g m}^{-3} \text{yr}^{-1}$ ; Fig. S4e), thus driving the BrC/BC ratio downward.

230 In addition, changes in anthropogenic emissions further enhance the declining BrC/BC ratio. Industrialization and urbanization have driven substantial growth in power plant emissions (Liu et al., 2023), while improved access to electricity has simultaneously reduced household combustion (Aleluia et al., 2022; Hoesly et al., 2018; Shyu, 2022). These changes result in a net increase in BC ( $+0.007 \mu\text{g m}^{-3} \text{yr}^{-1}$ ; Fig. S4e) and a decline in BrC ( $-0.008 \mu\text{g m}^{-3} \text{yr}^{-1}$ ; Fig. S4f).

Notably, the SHAP analysis identifies OBB as the dominant factor in modulating the BrC/BC mass ratio in Southeast Asia (Fig. 3f), though anthropogenically- and OBB-driven trends in BC and BrC have comparable magnitudes (Fig. 3c). It is because the substantially higher interannual variability of OBB, which is sensitive to climate events, makes it exert greater influence on the evolving BrC/BC ratio. More importantly, unlike wildfires at high northern latitudes, which exhibit a persistent increasing trend (Zheng et al., 2023; Zhong et al., 2024), OBB in Southeast Asia has experienced notable fluctuations associated with ENSO (Yin, 2020). These variations, in turn, can affect climate through interactions of LACs with radiation and clouds. This underscores the need for greater attention to regional fire-aerosol-climate interactions.

240

### 3.3 Radiative effects of BrC/BC trend

We evaluated the shortwave DRF of BC and BrC, as well as their ratio ( $\text{DRF}_{\text{BrC}}/\text{DRF}_{\text{BC}}$ ), over Asia from 2012 to 2019. Our estimates of  $\text{DRF}_{\text{BrC}}$  and  $\text{DRF}_{\text{BC}}$  over East, South and Southeast Asia are comparable to previous studies (Table S7). As shown in Fig. 4a, driven by changes in the BrC/BC mass ratio, the trend of  $\text{DRF}_{\text{BrC}}/\text{DRF}_{\text{BC}}$  also demonstrated significant spatial heterogeneity. East Asia exhibited a widespread and statistically significant positive trend, indicating the growing relative importance of BrC warming effect with respect to BC. In contrast, South and Southeast Asia showed a generally modest decline.

245

In East Asia, the  $\text{DRF}_{\text{BrC}}/\text{DRF}_{\text{BC}}$  increased from 34.1% in 2012 to 41.3% in 2019, driven by a decreasing  $\text{DRF}_{\text{BC}}$  ( $-0.20 \text{ W m}^{-2}$ , from  $1.09 \text{ W m}^{-2}$ ) alongside a relatively stable  $\text{DRF}_{\text{BrC}}$  ( $-0.005 \text{ W m}^{-2}$ , from  $0.37 \text{ W m}^{-2}$ ) (Fig. 4b). The modest change in  $\text{DRF}_{\text{BrC}}$  can be explained not only by the smaller decline in BrC concentrations (Fig. S4b), but also by the weaker absorption capacity of BrC compared to BC (Liu et al., 2015; Saleh, 2020). Anthropogenic emissions alone were responsible for larger declines in  $\text{DRF}_{\text{BC}}$  ( $-0.23 \text{ W m}^{-2}$ ) and  $\text{DRF}_{\text{BrC}}$  ( $-0.007 \text{ W m}^{-2}$ ). These results are comparable with recent estimates over China from 2014 to 2017 ( $-0.28$  and  $-0.018 \text{ W m}^{-2}$  in  $\text{DRF}_{\text{BC}}$  and  $\text{DRF}_{\text{BrC}}$ , respectively; Yang et al., 2024). However, despite being seasonal (You et al., 2026), increasing OBB emissions offset these anthropogenically driven reductions by 10.6% ( $\text{DRF}_{\text{BC}}$ ) and 28.6% ( $\text{DRF}_{\text{BrC}}$ ). These findings underscore the critical role of OBB in modulating the relative climate impacts of BrC and BC in this region.

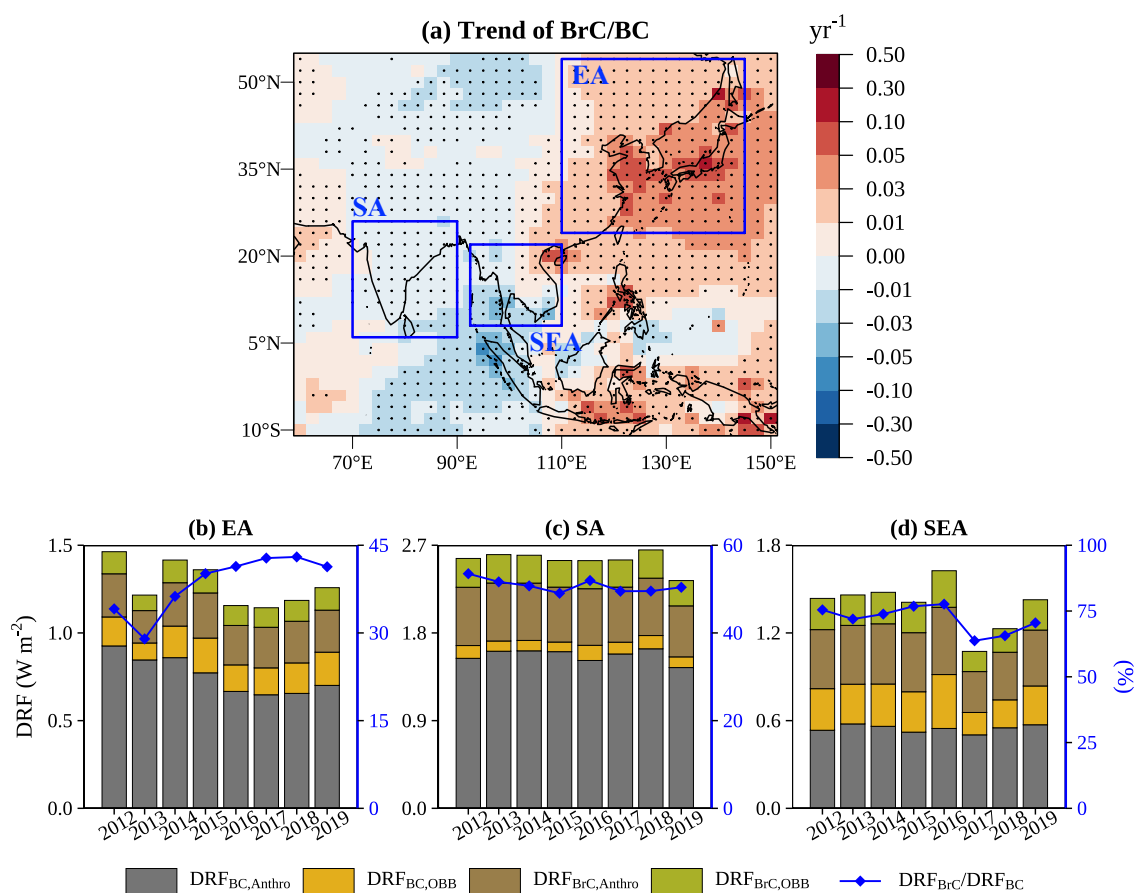
255

Conversely, the  $\text{DRF}_{\text{BrC}}/\text{DRF}_{\text{BC}}$  in South Asia decreased from 53.5% to 50.4%, caused by the larger decline in  $\text{DRF}_{\text{BrC}}$  compared to  $\text{DRF}_{\text{BC}}$  (Fig. 4c). This decline is driven by variations in anthropogenic emissions, particularly reductions in residential emissions (Gould and Urpelainen, 2018; Roy, 2024), in line with changes in its BrC/BC mass ratio (see Sect. 3.2.2 for details).

260



265 Southeast Asia, a wildfire hotspot, had the largest  $DRF_{BrC}/DRF_{BC}$  ( $> 70\%$ ) among the three regions, but this ratio decreased from 75.4% to 70.5% during 2012–2019 (Fig. 4d). This resulted from opposing changes in  $DRF_{BC}$  and  $DRF_{BrC}$ .  $DRF_{BC}$  increased due to growing anthropogenic emissions outweighing declining OBB emissions (Huang et al., 2024; Liu et al., 2023), whereas  $DRF_{BrC}$  decreased from reductions in both sources (Aleluia et al., 2022; Hoesly et al., 2018; Huang et al., 2024), as discussed in Sect. 3.2.3. Notably, OBB once again considerably modulated anthropogenically induced changes, with its decreasing emissions offsetting 50% of the  $DRF_{BC}$  increase and contributing 27.2% to the  $DRF_{BrC}$  reduction. Together with the findings in East Asia, these results highlight the substantial influence of OBB on regional climate forcing, despite its seasonal nature.



270 **Figure 4.** (a) Trends in  $DRF_{BrC}/DRF_{BC}$  across Asia for 2012–2019, with dots indicating statistical significance ( $p < 0.05$ ). East Asia (EA), South Asia (SA) and Southeast Asia (SEA) are outlined by blue rectangles. (b-d) Regional DRF of BC and BrC from anthropogenic ( $DRF_{BC,Anthro}$ ,  $DRF_{BrC,Anthro}$ ) and OBB sources ( $DRF_{BC,OBB}$ ,  $DRF_{BrC,OBB}$ ), and the corresponding  $DRF_{BrC}/DRF_{BC}$ .



#### 4. Conclusion

We investigated the responses of BC and BrC to profound variations in anthropogenic and open biomass burning emissions across Asia from 2012 to 2019, along with their key drivers, using the GEOS-Chem model combined with SHAP analysis. The corresponding changes in DRF of BC and BrC, alongside their relative contributions to the DRF of LACs, were also examined. East (policy-driven), South (near-baseline transition) and Southeast Asia (climate-sensitive) were analyzed in particular to inform mitigation strategies under different emission trajectories.

Our results reveal that emission mitigation does not uniformly reduce LACs loading across Asia, but instead drives a spatially heterogeneous redistribution of BC and BrC with distinct radiative consequences. In East Asia, rising OBB emissions from seasonal shifts in crop residue burning under open-fire restrictions slowed the anthropogenically driven declines in BC and BrC concentrations by 22.4% and 59.0%, respectively. Consequently, this elevated the BrC/BC mass ratio and enhanced the radiative importance of BrC, driving an increase in  $DRF_{BrC}/DRF_{BC}$  from 34.1% to 41.3%. In contrast, transitions to cleaner fuels and climate-driven wildfire variability drove opposing trends in South and Southeast Asia, respectively, where both the BrC/BC ratio and  $DRF_{BrC}/DRF_{BC}$  declined. Notably, in East and Southeast Asia, open burning accounted for up to half of the anthropogenically driven changes in radiative forcing of BC and BrC, underscoring its disproportionate influence on the regional energy budget despite its episodic and seasonal nature.

We note that these estimates are subject to uncertainties inherent in open burning emission inventories, which remain poorly constrained due to the high spatiotemporal variability of fire activity and fuel consumption (Pan et al., 2020; Xu et al., 2023b). Furthermore, the optical properties of BrC, particularly its wavelength-dependent absorption (Laskin et al., 2025; Saleh, 2020) and atmospheric aging-associated photobleaching (Laskin et al., 2025; Qiu et al., 2026), introduce additional uncertainty into radiative forcing estimates that warrants further observational and laboratory constraints. Nevertheless, these uncertainties do not weaken our findings. First, though open burning emissions remain uncertain, their trends are consistent across multiple inventories (Liu et al., 2026). Thus, the simulated trends of OBB-emitted BC and BrC, and their influence on the BrC/BC mass ratio, are robust. Second, photobleaching indeed reduces BrC absorption and may affect the instantaneous  $DRF_{BrC}/DRF_{BC}$  ratio, but its impact on the multi-year trend of this ratio is limited, because this effect is unlikely to vary substantially across years. Finally, concentrations of BC and OC, absorption coefficients of BrC, and trends in OBB-emitted BC and BrC are validated against observations. All show good agreement, further supporting the robustness of our results.

Therefore, our results suggest that the open burning, spanning both policy-regulated agricultural burning and climate-sensitive wildfires, plays an increasingly important role in Asia's aerosol-climate system, as clean air policies effectively suppress anthropogenic emissions. Achieving co-benefits for air quality and climate will therefore require integrated management strategies that address open burning in parallel with ongoing anthropogenic emission controls.



### Code and data availability

The GEOS-Chem model is publicly available at <https://github.com/geoschem/>, and the version we used (v.13.2.0) can be  
305 found at <http://10.5281/zenodo.5500536>. The RRTMG\_SW model is publicly available at [https://github.com/AER-RC/RRTMG\\_SW](https://github.com/AER-RC/RRTMG_SW). Observation of BC mass concentration at Fukue is available at <https://www.jamstec.go.jp/egcr/e/atmos/observation/topics1.html>; other observations of BC and OC mass concentrations are obtained from previous studies, as indicated in the text. Observations of BrC absorption are obtained from previous studies and in-situ measurements, as indicated in the text. Satellite-retrieved burned area is obtained from t <https://doi.org/10.5281/zenodo.7668423> (Chen et al.,  
310 2023).

### Author contributions

YZ: data curation, formal analysis, writing (original draft preparation). AA: data curation, writing (original draft preparation).  
YLZ: conceptualization, writing (review and editing).

### Competing interests

315 The contact author has declared that none of the authors has any competing interests.

### Acknowledgements

The authors gratefully acknowledge the financial support of the National Natural Science Foundation of China, and the technical support of the National Large Scientific and Technological Infrastructure “Earth System Numerical Simulation Facility” (<https://cstr.cn/31134.02.EL>).

### 320 Financial support

This work was financially supported by the National Natural Science Foundation of China (Grant Nos. 42325304).

### References

- 325 Abulimiti, A., Zhang, Y., Yu, M., Hong, Y., Lin, Y.-C., Gul, C., and Cao, F.: Sources and trends of black carbon aerosol in the megacity of Nanjing, eastern China, after the China Clean Action Plan and Three-Year Action Plan, *Atmos. Chem. Phys.*, 25, 6161–6178, <https://doi.org/10.5194/acp-25-6161-2025>, 2025.
- Aleluia, J., Tharakan, P., Chikkatur, A. P., Shrimali, G., and Chen, X.: Accelerating a clean energy transition in Southeast Asia: Role of governments and public policy, *Renewable and Sustainable Energy Reviews*, 159, 112226, <https://doi.org/10.1016/j.rser.2022.112226>, 2022.



- 330 Atwi, K., Cheng, Z., El Hajj, O., Perrie, C., and Saleh, R.: A dominant contribution to light absorption by methanol-insoluble brown carbon produced in the combustion of biomass fuels typically consumed in wildland fires in the United States, *Environmental Science: Atmospheres*, 2, 182–191, <https://doi.org/10.1039/d1ea00065a>, 2022.
- Bhuvaneshwari, S., Hettiarachchi, H., and Meegoda, J. N.: Crop Residue Burning in India: Policy Challenges and Potential Solutions, *IJERPH*, 16, 832, <https://doi.org/10.3390/ijerph16050832>, 2019.
- 335 Biswal, A., Katoch, V., Singh, T., Ravindra, K., Singh, V., and Mor, S.: Changing tropospheric NO<sub>2</sub> dynamics across Indian air pollution hotspots, *Environmental Pollution*, 373, 126160, <https://doi.org/10.1016/j.envpol.2025.126160>, 2025.
- Bond, T. C. and Bergstrom, R. W.: Light Absorption by Carbonaceous Particles: An Investigative Review, *Aerosol Science and Technology*, 40, 27–67, <https://doi.org/10.1080/02786820500421521>, 2006.
- 340 Bond, T. C., Doherty, S. J., Fahey, D. W., Forster, P. M., Berntsen, T., DeAngelo, B. J., Flanner, M. G., Ghan, S., Kärcher, B., Koch, D., Kinne, S., Kondo, Y., Quinn, P. K., Sarofim, M. C., Schultz, M. G., Schulz, M., Venkataraman, C., Zhang, H., Zhang, S., Bellouin, N., Guttikunda, S. K., Hopke, P. K., Jacobson, M. Z., Kaiser, J. W., Klimont, Z., Lohmann, U., Schwarz, J. P., Shindell, D., Storelvmo, T., Warren, S. G., and Zender, C. S.: Bounding the role of black carbon in the climate system: A scientific assessment, *Journal of Geophysical Research: Atmospheres*, 118, 5380–5552, <https://doi.org/10.1002/jgrd.50171>, 2013.
- 345 Chatterjee, D., McDuffie, E. E., Smith, S. J., Bindle, L., Van Donkelaar, A., Hammer, M. S., Venkataraman, C., Brauer, M., and Martin, R. V.: Source Contributions to Fine Particulate Matter and Attributable Mortality in India and the Surrounding Region, *Environ. Sci. Technol.*, 57, 10263–10275, <https://doi.org/10.1021/acs.est.2c07641>, 2023.
- Chen, D., Zhao, Y., Lyu, R., Wu, R., Dai, L., Zhao, Y., Chen, F., Zhang, J., Yu, H., and Guan, M.: Seasonal and spatial variations of optical properties of light absorbing carbon and its influencing factors in a typical polluted city in Yangtze River Delta, China, *Atmospheric Environment*, 199, 45–54, <https://doi.org/10.1016/j.atmosenv.2018.11.022>, 2019.
- 350 Chen, Y., Morton, D. C., Andela, N., Van Der Werf, G. R., Giglio, L., and Randerson, J. T.: A pan-tropical cascade of fire driven by El Niño/Southern Oscillation, *Nature Clim Change*, 7, 906–911, <https://doi.org/10.1038/s41558-017-0014-8>, 2017.
- 355 Chen, Y., Hall, J., Van Wees, D., Andela, N., Hantson, S., Giglio, L., Van Der Werf, G. R., Morton, D. C., and Randerson, J. T.: Multi-decadal trends and variability in burned area from the fifth version of the Global Fire Emissions Database (GFED5), *Earth Syst. Sci. Data*, 15, 5227–5259, <https://doi.org/10.5194/essd-15-5227-2023>, 2023.
- Cleveland, R. B., Cleveland, W. S., McRae, J. E., Terpenning, I., and others: STL: A seasonal-trend decomposition, *Journal of Official Statistics*, 6, 3–73, 1990.
- 360 Dai, T., Dai, Q., Ding, J., Liu, B., Bi, X., Wu, J., Zhang, Y., and Feng, Y.: Measuring the emission changes and meteorological dependence of source-specific BC aerosol using factor analysis coupled with machine learning, *Journal of Geophysical Research: Atmospheres*, 128, e2023JD038696, 2023.
- DeLessio, M. A., Tsigaridis, K., Bauer, S. E., Chowdhary, J., and Schuster, G. L.: Modeling atmospheric brown carbon in the GISS ModelE Earth system model, *Atmospheric Chemistry and Physics*, 24, 6275–6304, <https://doi.org/10.5194/acp-24-6275-2024>, 2024.
- 365 Dong, L., Long, X., Wang, Z., Xie, M., Han, X., Cao, J., Dong, Z., Yang, J., and Wang, Y.: Spatiotemporal variations of farmland crop residue burning in China from 2013 to 2022, *Science of The Total Environment*, 954, 176647, <https://doi.org/10.1016/j.scitotenv.2024.176647>, 2024.



- Drugé, T., Nabat, P., Mallet, M., Michou, M., Rémy, S., and Dubovik, O.: Modeling radiative and climatic effects of brown carbon aerosols with the ARPEGE-Climat global climate model, *Atmospheric Chemistry and Physics*, 22, 12167–12205, <https://doi.org/10.5194/acp-22-12167-2022>, 2022.
- 370 Geng, G., Liu, Y., Liu, Y., Liu, S., Cheng, J., Yan, L., Wu, N., Hu, H., Tong, D., and Zheng, B.: Efficacy of China’s clean air actions to tackle PM<sub>2.5</sub> pollution between 2013 and 2020, *Nature Geoscience*, 17, 987–994, 2024.
- Gong, X., Liu, Z., Tian, J., Wang, Q., Li, G., An, Z., and Han, Y.: Spatiotemporal patterns and drivers of wildfire CO<sub>2</sub> emissions in China from 2001 to 2022, *Atmos. Chem. Phys.*, 25, 10379–10401, <https://doi.org/10.5194/acp-25-10379-2025>, 2025.
- 375 Gould, C. F. and Urpelainen, J.: LPG as a clean cooking fuel: Adoption, use, and impact in rural India, *Energy Policy*, 122, 395–408, <https://doi.org/10.1016/j.enpol.2018.07.042>, 2018.
- Guenther, A. B., Jiang, X., Heald, C. L., Sakulyanontvittaya, T., Duhl, T., Emmons, L. K., and Wang, X.: The Model of Emissions of Gases and Aerosols from Nature version 2.1 (MEGAN2.1): an extended and updated framework for modeling biogenic emissions, *Geoscientific Model Development*, 5, 1471–1492, <https://doi.org/10.5194/gmd-5-1471-2012>, 2012.
- 380 He, C., Niu, X., Ye, Z., Wu, Q., Liu, L., Zhao, Y., Ni, J., Li, B., and Jin, J.: Black carbon pollution in China from 2001 to 2019: Patterns, trends, and drivers, *Environmental Pollution*, 324, 121381, <https://doi.org/10.1016/j.envpol.2023.121381>, 2023.
- Hoesly, R. M., Smith, S. J., Feng, L., Klimont, Z., Janssens-Maenhout, G., Pitkanen, T., Seibert, J. J., Vu, L., Andres, R. J., Bolt, R. M., Bond, T. C., Dawidowski, L., Kholod, N., Kurokawa, J., Li, M., Liu, L., Lu, Z., Moura, M. C. P., O’Rourke, P. R., and Zhang, Q.: Historical (1750–2014) anthropogenic emissions of reactive gases and aerosols from the Community Emissions Data System (CEDS), *Geoscientific Model Development*, 11, 369–408, <https://doi.org/10.5194/gmd-11-369-2018>, 2018.
- 385 Hou, L., Dai, Q., Song, C., Liu, B., Guo, F., Dai, T., Li, L., Liu, B., Bi, X., Zhang, Y., and others: Revealing drivers of haze pollution by explainable machine learning, *Environmental Science & Technology Letters*, 9, 112–119, 2022.
- 390 Hu, Y., Yue, X., and Tian, C.: Impacts of El Niño–Southern Oscillation on global fire PM<sub>2.5</sub> during 2000–2023, *Atmospheric and Oceanic Science Letters*, 18, 100597, <https://doi.org/10.1016/j.aosl.2025.100597>, 2025.
- Huang, H.-Y., Wang, S.-H., Lau, W. K., Wang, S.-Y. S., and da Silva, A. M.: Impact of regional climate patterns on the biomass burning emissions and transport over Peninsular Southeast Asia, 2000–2019, *Atmospheric Research*, 297, 107067, 2024.
- 395 Iacono, M. J., Delamere, J. S., Mlawer, E. J., Shephard, M. W., Clough, S. A., and Collins, W. D.: Radiative forcing by long-lived greenhouse gases: Calculations with the AER radiative transfer models, *Journal of Geophysical Research: Atmospheres*, 113, <https://doi.org/10.1029/2008JD009944>, 2008.
- 400 Ichoku, C. and Ellison, L.: Global top-down smoke-aerosol emissions estimation using satellite fire radiative power measurements, *Atmospheric Chemistry and Physics*, 14, 6643–6667, <https://doi.org/10.5194/acp-14-6643-2014>, 2014.
- IPCC: Climate Change 2021: The Physical Science Basis. Contribution of Working Group I to the Sixth Assessment Report of the Intergovernmental Panel on Climate Change, Cambridge University Press, 2021.



- 405 Ji, D., Gao, W., Maenhaut, W., He, J., Wang, Z., Li, J., Du, W., Wang, L., Sun, Y., Xin, J., Hu, B., and Wang, Y.: Impact of air pollution control measures and regional transport on carbonaceous aerosols in fine particulate matter in urban Beijing, China: insights gained from long-term measurement, *Atmos. Chem. Phys.*, 19, 8569–8590, <https://doi.org/10.5194/acp-19-8569-2019>, 2019.
- Jo, D. S., Park, R. J., Lee, S., Kim, S.-W., and Zhang, X.: A global simulation of brown carbon: implications for photochemistry and direct radiative effect, *Atmospheric Chemistry and Physics*, 16, 3413–3432, <https://doi.org/10.5194/acp-16-3413-2016>, 2016.
- 410 Jones, M. W., Abatzoglou, J. T., Veraverbeke, S., Andela, N., Lasslop, G., Forkel, M., Smith, A. J. P., Burton, C., Betts, R. A., Van Der Werf, G. R., Sitch, S., Canadell, J. G., Santin, C., Kolden, C., Doerr, S. H., and Le Quéré, C.: Global and Regional Trends and Drivers of Fire Under Climate Change, *Reviews of Geophysics*, 60, e2020RG000726, <https://doi.org/10.1029/2020RG000726>, 2022.
- 415 Kanaya, Y., Yamaji, K., Miyakawa, T., Taketani, F., Zhu, C., Choi, Y., Komazaki, Y., Ikeda, K., Kondo, Y., and Klimont, Z.: Rapid reduction in black carbon emissions from China: evidence from 2009–2019 observations on Fukue Island, Japan, *Atmospheric Chemistry and Physics*, 20, 6339–6356, 2020.
- Kim, P. S., Jacob, D. J., Fisher, J. A., Travis, K., Yu, K., Zhu, L., Yantosca, R. M., Sulprizio, M. P., Jimenez, J. L., Campuzano-Jost, P., Froyd, K. D., Liao, J., Hair, J. W., Fenn, M. A., Butler, C. F., Wagner, N. L., Gordon, T. D., Welti, A., Wennberg, P. O., Crouse, J. D., St. Clair, J. M., Teng, A. P., Millet, D. B., Schwarz, J. P., Markovic, M. Z., and Perring, A. E.: Sources, seasonality, and trends of southeast US aerosol: an integrated analysis of surface, aircraft, and satellite observations with the GEOS-Chem chemical transport model, *Atmospheric Chemistry and Physics*, 15, 10411–10433, <https://doi.org/10.5194/acp-15-10411-2015>, 2015.
- 420 Kirchstetter, T. W., Novakov, T., and Hobbs, P. V.: Evidence that the spectral dependence of light absorption by aerosols is affected by organic carbon, *Journal of Geophysical Research: Atmospheres*, 109, D21208, <https://doi.org/10.1029/2004jd004999>, 2004.
- 425 Koukouli, M. E., Theys, N., Ding, J., Zyrichidou, I., Mijling, B., Balis, D., and van der A, R. J.: Updated SO<sub>2</sub> emission estimates over China using OMI/Aura observations, *Atmospheric Measurement Techniques*, 11, 1817–1832, <https://doi.org/10.5194/amt-11-1817-2018>, 2018.
- Kurokawa, J. and Ohara, T.: Long-term historical trends in air pollutant emissions in Asia: Regional Emission inventory in ASia (REAS) version 3, *Atmos. Chem. Phys.*, 20, 12761–12793, <https://doi.org/10.5194/acp-20-12761-2020>, 2020.
- 430 Laskin, A., West, C. P., and Hettiyadura, A. P. S.: Molecular insights into the composition, sources, and aging of atmospheric brown carbon, *Chem. Soc. Rev.*, 54, 1583–1612, <https://doi.org/10.1039/D3CS00609C>, 2025.
- 435 Li, L., Qian, J., Ou, C.-Q., Zhou, Y.-X., Guo, C., and Guo, Y.: Spatial and temporal analysis of Air Pollution Index and its timescale-dependent relationship with meteorological factors in Guangzhou, China, 2001–2011, *Environmental pollution*, 190, 75–81, 2014.
- Li, S., Wang, S., Wu, Q., Zhang, Y., Ouyang, D., Zheng, H., Han, L., Qiu, X., Wen, Y., Liu, M., Jiang, Y., Yin, D., Liu, K., Zhao, B., Zhang, S., Wu, Y., and Hao, J.: Emission trends of air pollutants and CO<sub>2</sub> in China from 2005 to 2021, *Earth Syst. Sci. Data*, 15, 2279–2294, <https://doi.org/10.5194/essd-15-2279-2023>, 2023.
- 440 Liu, B., Guan, Y., Shan, Y., Cui, C., and Hubacek, K.: Emission growth and drivers in Mainland Southeast Asian countries, *Journal of Environmental Management*, 329, 117034, <https://doi.org/10.1016/j.jenvman.2022.117034>, 2023.



- Liu, D., He, C., Schwarz, J. P., and Wang, X.: Lifecycle of light-absorbing carbonaceous aerosols in the atmosphere, *npj Climate and Atmospheric Science*, 3, <https://doi.org/10.1038/s41612-020-00145-8>, 2020.
- 445 Liu, P. F., Abdelmalki, N., Hung, H. M., Wang, Y., Brune, W. H., and Martin, S. T.: Ultraviolet and visible complex refractive indices of secondary organic material produced by photooxidation of the aromatic compounds toluene and *m*-xylene, *Atmospheric Chemistry and Physics*, 15, 1435–1446, <https://doi.org/10.5194/acp-15-1435-2015>, 2015.
- Liu, S., Geng, G., Xiao, Q., Zheng, Y., Liu, X., Cheng, J., and Zhang, Q.: Tracking Daily Concentrations of PM(2.5) Chemical Composition in China since 2000, *Environmental Science & Technology*, 56, 16517–16527, <https://doi.org/10.1021/acs.est.2c06510>, 2022a.
- 450 Liu, X., Sun, Z., Shi, C., Wang, P., Nie, T., Chu, Q., Shang, H., Sun, L., Ji, D., Guo, M., Yi, K., Tan, Z., Wu, L., Lu, X., and Yin, S.: The newly developed Multi-ensemble Biomass-burning Emissions Inventory (MBEI): characterizing and unraveling spatiotemporal uncertainty in global biomass burning emissions, *Earth Syst. Sci. Data*, 18, 1203–1224, <https://doi.org/10.5194/essd-18-1203-2026>, 2026.
- Liu, Y., Zhao, H., Zhao, G., Zhang, X., and Xiu, A.: Carbonaceous gas and aerosol emissions from biomass burning in China from 2012 to 2021, *Journal of Cleaner Production*, 362, 132199, <https://doi.org/10.1016/j.jclepro.2022.132199>, 2022b.
- 455 Majumdar, D.: Spatial distribution and temporal variation of biomass burning and surface black carbon concentrations during summer (2015–2021) in India, *Air Qual Atmos Health*, 16, 459–476, <https://doi.org/10.1007/s11869-022-01284-y>, 2023.
- Martin, R. V., Jacob, D. J., Yantosca, R. M., Chin, M., and Ginoux, P.: Global and regional decreases in tropospheric oxidants from photochemical effects of aerosols, *Journal of Geophysical Research: Atmospheres*, 108, 4097, <https://doi.org/10.1029/2002jd002622>, 2003.
- 460 McDuffie, E. E., Smith, S. J., O'Rourke, P., Tibrewal, K., Venkataraman, C., Marais, E. A., Zheng, B., Crippa, M., Brauer, M., and Martin, R. V.: A global anthropogenic emission inventory of atmospheric pollutants from sector- and fuel-specific sources (1970–2017): an application of the Community Emissions Data System (CEDS), *Earth System Science Data*, 12, 3413–3442, <https://doi.org/10.5194/essd-12-3413-2020>, 2020.
- 465 Pan, X., Ichoku, C., Chin, M., Bian, H., Darmenov, A., Colarco, P., Ellison, L., Kucsera, T., da Silva, A., Wang, J., Oda, T., and Cui, G.: Six global biomass burning emission datasets: intercomparison and application in one global aerosol model, *Atmospheric Chemistry and Physics*, 20, 969–994, <https://doi.org/10.5194/acp-20-969-2020>, 2020.
- Park, R. J., Jacob, D. J., Chin, M., and Martin, R. V.: Sources of carbonaceous aerosols over the United States and implications for natural visibility, *Journal of Geophysical Research: Atmospheres*, 108, 4355, <https://doi.org/10.1029/2002jd003190>, 2003.
- 470 Pathak, M., Kuttippurath, J., and Kumar, R.: Long-term changes in black carbon aerosols and their health effects in rural India during the past two decades (2000–2019), *Journal of Hazardous Materials Advances*, 16, 100519, <https://doi.org/10.1016/j.hazadv.2024.100519>, 2024.
- 475 Qiu, Y., Qiu, T., Wu, Z., Liu, Y., Fang, W., Man, R., Liu, Y., Wang, J., Meng, X., Chen, J., Liang, D., Guo, S., and Hu, M.: Observational Evidence of Brown Carbon Photobleaching in Urban Atmosphere at Molecular Level, *Environ. Sci. Technol. Lett.*, 11, 1032–1039, <https://doi.org/10.1021/acs.estlett.4c00647>, 2024.



- Qiu, Y., Qiu, T., Liu, Y., Gu, Y., Man, R., Liang, D., Zong, T., Wu, Z., and Hu, M.: Understanding divergent brown carbon photobleaching rates from molecular perspective, *Atmos. Chem. Phys.*, 26, 2785–2796, <https://doi.org/10.5194/acp-26-2785-2026>, 2026.
- 480 Reddington, C. L., Conibear, L., Knote, C., Silver, B. J., Li, Y. J., Chan, C. K., Arnold, S. R., and Spracklen, D. V.: Exploring the impacts of anthropogenic emission sectors on PM<sub>2.5</sub> and human health in South and East Asia, *Atmos. Chem. Phys.*, 19, 11887–11910, <https://doi.org/10.5194/acp-19-11887-2019>, 2019.
- Roy, K.: Transition to cooking with clean fuels in rural households of India: Studying the effect of policy and other factors, *Energy for Sustainable Development*, 80, 101456, <https://doi.org/10.1016/j.esd.2024.101456>, 2024.
- 485 Saleh, R.: From Measurements to Models: Toward Accurate Representation of Brown Carbon in Climate Calculations, *Current Pollution Reports*, 6, 90–104, <https://doi.org/10.1007/s40726-020-00139-3>, 2020.
- Saleh, R., Marks, M., Heo, J., Adams, P. J., Donahue, N. M., and Robinson, A. L.: Contribution of brown carbon and lensing to the direct radiative effect of carbonaceous aerosols from biomass and biofuel burning emissions, *Journal of Geophysical Research: Atmospheres*, 120, 10285–10296, <https://doi.org/10.1002/2015jd023697>, 2015.
- 490 Sand, M., Samset, B. H., Myhre, G., Glib, J., Bauer, S. E., Bian, H., Chin, M., Checa-Garcia, R., Ginoux, P., Kipling, Z., Kirkevåg, A., Kokkola, H., Le Sager, P., Lund, M. T., Matsui, H., van Noije, T., Olivié, D. J. L., Remy, S., Schulz, M., Stier, P., Stjern, C. W., Takemura, T., Tsigaridis, K., Tsyro, S. G., and Watson-Parris, D.: Aerosol absorption in global models from AeroCom phase III, *Atmospheric Chemistry and Physics*, 21, 15929–15947, <https://doi.org/10.5194/acp-21-15929-2021>, 2021.
- 495 Satish, R., Rastogi, N., Singh, A., and Singh, D.: Change in characteristics of water-soluble and water-insoluble brown carbon aerosols during a large-scale biomass burning, *Environ Sci Pollut Res*, 27, 33339–33350, <https://doi.org/10.1007/s11356-020-09388-7>, 2020.
- Sharma, V. and Dash, M.: Household energy use pattern in rural India: A path towards sustainable development, *Environmental Challenges*, 6, 100404, <https://doi.org/10.1016/j.envc.2021.100404>, 2022.
- 500 Shyu, C.-W.: Energy poverty alleviation in Southeast Asian countries: Policy implications for improving access to electricity, *Journal of Asian Public Policy*, 15, 97–121, 2022.
- Siemens, K., Morales, A., He, Q., Li, C., Hettiyadura, A. P. S., Rudich, Y., and Laskin, A.: Molecular Analysis of Secondary Brown Carbon Produced from the Photooxidation of Naphthalene, *Environ. Sci. Technol.*, 56, 3340–3353, <https://doi.org/10.1021/acs.est.1c03135>, 2022.
- 505 Sun, J., Wang, Z., Zhou, W., Xie, C., Wu, C., Chen, C., Han, T., Wang, Q., Li, Z., Li, J., Fu, P., Wang, Z., and Sun, Y.: Measurement report: Long-term changes in black carbon and aerosol optical properties from 2012 to 2020 in Beijing, China, *Atmos. Chem. Phys.*, 22, 561–575, <https://doi.org/10.5194/acp-22-561-2022>, 2022.
- Thornhill, G. D., Collins, W. J., Kramer, R. J., Olivié, D., Skeie, R. B., O'Connor, F. M., Abraham, N. L., Checa-Garcia, R., Bauer, S. E., Deushi, M., Emmons, L. K., Forster, P. M., Horowitz, L. W., Johnson, B., Keeble, J., Lamarque, J.-F., Michou, M., Mills, M. J., Mulcahy, J. P., Myhre, G., Nabat, P., Naik, V., Oshima, N., Schulz, M., Smith, C. J., Takemura, T., Tilmes, S., Wu, T., Zeng, G., and Zhang, J.: Effective radiative forcing from emissions of reactive gases and aerosols – a multi-model comparison, *Atmospheric Chemistry and Physics*, 21, 853–874, <https://doi.org/10.5194/acp-21-853-2021>, 2021.



- 515 Tuccella, P., Curci, G., Pitari, G., Lee, S., and Jo, D. S.: Direct Radiative Effect of Absorbing Aerosols: Sensitivity to Mixing State, Brown Carbon, and Soil Dust Refractive Index and Shape, *Journal of Geophysical Research: Atmospheres*, 125, e2019JD030967, <https://doi.org/10.1029/2019jd030967>, 2020.
- Wang, L., Jin, X., Wang, Q., Mao, H., Liu, Q., Weng, G., and Wang, Y.: Spatial and temporal variability of open biomass burning in Northeast China from 2003 to 2017, *Atmospheric and Oceanic Science Letters*, 13, 240–247, <https://doi.org/10.1080/16742834.2020.1742574>, 2020.
- 520 Wang, Q., Zhou, Y., Ma, N., Zhu, Y., Zhao, X., Zhu, S., Tao, J., Hong, J., Wu, W., Cheng, Y., and Su, H.: Review of Brown Carbon Aerosols in China: Pollution Level, Optical Properties, and Emissions, *Journal of Geophysical Research: Atmospheres*, 127, e2021JD035473, <https://doi.org/10.1029/2021JD035473>, 2022.
- 525 Wang, Y., Huang, R.-J., Zhong, H., Wang, T., Yang, L., Yuan, W., Xu, W., and An, Z.: Predictions of the Optical Properties of Brown Carbon Aerosol by Machine Learning with Typical Chromophores, *Environmental Science & Technology*, 58, 20588–20597, <https://doi.org/10.1021/acs.est.4c09031>, 2024.
- Wong, J. P. S., Nenes, A., and Weber, R. J.: Changes in Light Absorptivity of Molecular Weight Separated Brown Carbon Due to Photolytic Aging, *Environ. Sci. Technol.*, 51, 8414–8421, <https://doi.org/10.1021/acs.est.7b01739>, 2017.
- 530 Xie, X., Chen, Y., Nie, D., Liu, Y., Liu, Y., Lei, R., Zhao, X., Li, H., and Ge, X.: Light-absorbing and fluorescent properties of atmospheric brown carbon: A case study in Nanjing, China, *Chemosphere*, 251, 126350, <https://doi.org/10.1016/j.chemosphere.2020.126350>, 2020.
- Xie, Y., Zeng, L., Hu, S., Wang, T., Du, Z., Tan, T., Xu, N., Chen, S., Mao, J., Xu, F., and Hu, M.: Long-term trends of black carbon levels, sources, and radiative effects from 2013 to 2022 in Beijing, China, *npj Clean Air*, 1, 10, <https://doi.org/10.1038/s44407-025-00010-z>, 2025.
- 535 Xiong, R., Li, J., Zhang, Y., Zhang, L., Jiang, K., Zheng, H., Kong, S., Shen, H., Cheng, H., Shen, G., and Tao, S.: Global brown carbon emissions from combustion sources, *Environmental Science and Ecotechnology*, 12, 100201, <https://doi.org/10.1016/j.ese.2022.100201>, 2022.
- Xu, H., Ren, Y., Zhang, W., Meng, W., Yun, X., Yu, X., Li, J., Zhang, Y., Shen, G., Ma, J., Li, B., Cheng, H., Wang, X., Wan, Y., and Tao, S.: Updated Global Black Carbon Emissions from 1960 to 2017: Improvements, Trends, and Drivers, *Environ. Sci. Technol.*, 55, 7869–7879, <https://doi.org/10.1021/acs.est.1c03117>, 2021.
- 540 Xu, L., Ou, Y., Cai, J., Wang, J., Fu, Y., and Bian, X.: Offshore wind speed assessment with statistical and attention-based neural network methods based on STL decomposition, *Renewable Energy*, 216, 119097, 2023a.
- Xu, L., Lin, G., Liu, X., Wu, C., Wu, Y., and Lou, S.: Constraining Light Absorption of Brown Carbon in China and Implications for Aerosol Direct Radiative Effect, *Geophysical Research Letters*, 51, e2024GL109861, <https://doi.org/10.1029/2024GL109861>, 2024.
- 545 Xu, Y., Huang, Z., Ye, J., and Zheng, J.: Hourly emissions of air pollutants and greenhouse gases from open biomass burning in China during 2016–2020, *Scientific Data*, 10, <https://doi.org/10.1038/s41597-023-02541-0>, 2023b.
- Yadav, I. C., Linthoingambi Devi, N., Li, J., Syed, J. H., Zhang, G., and Watanabe, H.: Biomass burning in Indo-China peninsula and its impacts on regional air quality and global climate change—a review, *Environmental Pollution*, 227, 414–427, <https://doi.org/10.1016/j.envpol.2017.04.085>, 2017.



- 550 Yang, L., Mao, Y., Liao, H., Xie, M., and Zhang, Y.: Direct radiative forcing of light-absorbing carbonaceous aerosols in China, *Atmospheric Research*, 304, 107396, 2024.
- Yin, S.: Biomass burning spatiotemporal variations over South and Southeast Asia, *Environment International*, 145, 106153, <https://doi.org/10.1016/j.envint.2020.106153>, 2020.
- 555 Yin, S., Guo, M., Wang, X., Yamamoto, H., and Ou, W.: Spatiotemporal variation and distribution characteristics of crop residue burning in China from 2001 to 2018, *Environmental Pollution*, 268, 115849, <https://doi.org/10.1016/j.envpol.2020.115849>, 2021.
- You, C., Wang, J., Dong, X., and Xu, C.: Burning Bans Have Altered Burned Area Changes in China Since 2003, *Geophysical Research Letters*, 53, e2025GL120528, <https://doi.org/10.1029/2025GL120528>, 2026.
- 560 Zhang, A., Wang, Y., Zhang, Y., Weber, R. J., Song, Y., Ke, Z., and Zou, Y.: Modeling the global radiative effect of brown carbon: a potentially larger heating source in the tropical free troposphere than black carbon, *Atmospheric Chemistry and Physics*, 20, 1901–1920, <https://doi.org/10.5194/acp-20-1901-2020>, 2020.
- Zheng, B., Tong, D., Li, M., Liu, F., Hong, C., Geng, G., Li, H., Li, X., Peng, L., Qi, J., Yan, L., Zhang, Y., Zhao, H., Zheng, Y., He, K., and Zhang, Q.: Trends in China’s anthropogenic emissions since 2010 as the consequence of clean air actions, *Atmospheric Chemistry and Physics*, 18, 14095–14111, <https://doi.org/10.5194/acp-18-14095-2018>, 2018.
- 565 Zheng, B., Ciais, P., Chevallier, F., Yang, H., Canadell, J. G., Chen, Y., Van Der Velde, I. R., Aben, I., Chuvieco, E., Davis, S. J., Deeter, M., Hong, C., Kong, Y., Li, H., Li, H., Lin, X., He, K., and Zhang, Q.: Record-high CO<sub>2</sub> emissions from boreal fires in 2021, *Science*, 379, 912–917, <https://doi.org/10.1126/science.ade0805>, 2023.
- Zheng, H., Kong, S., Ding, D., Savadkoochi, M., Song, C., Zheng, M., and Harrison, R. M.: Black carbon aerosols in China: spatial-temporal variations and lessons from long-term atmospheric observations, *Atmos. Chem. Phys.*, 25, 16363–16386, <https://doi.org/10.5194/acp-25-16363-2025>, 2025.
- 570 Zhong, Q., Schutgens, N., Veraverbeke, S., and Van Der Werf, G. R.: Increasing aerosol emissions from boreal biomass burning exacerbate Arctic warming, *Nat. Clim. Chang.*, 14, 1275–1281, <https://doi.org/10.1038/s41558-024-02176-y>, 2024.
- 575 Zhou, Y., Zhang, W., Lang, J., Li, X., Zheng, X., Yang, C., Huang, R., Chen, D., and Cheng, S.: Spatiotemporal Dynamics and Key Drivers of Brown Carbon Emissions from Biomass Burning in China: A Historical to Future Perspective (1980–2035), *Environ. Sci. Technol.*, 60, 6177–6187, <https://doi.org/10.1021/acs.est.5c15482>, 2026.